Efficacy of diffusion-weighted magnetic resonance imaging in the head and neck region

頭頸部領域における拡散強調 MR 画像の有用性

日本大学大学院松戸歯学研究科

放射線学

大塚　航平

（指導：　金田　隆　教授）

本論文は、

1. Evaluation of the mandibular canal on inflammatory condition by magnetic resonance imaging

   International Journal of Oral-Medical Sciences (in press)

2. Quantitative analysis of age-related changes in cervical lymph nodes using diffusion-weighted imaging

   Journal of Oral and Maxillofacial Surgery, Medicine, and Pathology（第 38 巻 3 号 令和 4 年 10 月発行）

をまとめたものである。

1. Abstract

Purposes:

The purposes of this study were 1) to evaluate of the mandibular canal (MC) on inflammatory condition using magnetic resonance imaging (MRI), 2) to investigate age-related changes in apparent diffusion coefficient (ADC) values of cervical lymph node using diffusion-weighted imaging (DWI).

Materials and Methods:

1) The present study conducted a retrospective study of osteomyelitis patient who underwent MRI between August 2013 and March 2020. The participants comprised 130 patients (50 men, 80 women; age range, 20–89 years; mean age, 55.7 years). The Wilcoxon signed-rank test was used to compare the ADC values of the MC on the affected and non-affected sides. This test was performed using the ADC value of the MC as the criterion variable and disease status as the explanatory variable.

2) The present study conducted a retrospective study of patients who underwent pantomography and MRI between November 2017 and July 2018. The participants comprised 101 patients with 389 nodes (22 men, 79 women; age range, 14–77 years; mean age, 44.33 years). The correlation between the age group of the criterion variable and ADC value of the explanatory variable was analyzed using Spearman's correlation coefficient.

Results:

1) The median ADC value of the MC on the affected side was 1.34×10^{-3} mm^2/s and that of the MC on the non-affected side was 1.12×10^{-3} mm^2/s. The median ADC value of the MC affected side were higher than those of the non-affected side ($P<0.01$).

2) Significant negative correlation between age and the ADC values for each sex ($P < 0.001$). The mean ADC value of the submandibular nodes for all age groups was $0.88 \pm 0.15\times10^{-3}$ mm^2/s in men and $0.83 \pm 0.12\times10^{-3}$ mm^2/s in women ($P= 0.211$). The mean ADC value of the superior internal jugular nodes for all age groups was $0.90 \pm 0.14 \times10^{-3}$ mm^2/s in men and $0.91 \pm 0.16 \times10^{-3}$ mm^2/s in women ($P = 0.857$).

Conclusion:

The present study found that 1) the ADC value of MC affected by osteomyelitis was significantly higher than theses of the MC non-affected side, 2) the normal ADC values of cervical lymph nodes exhibited significant negative correlation with increasing age. These results suggested the efficacy of DWI in the head and neck region.

Key Words: mandibular canal, osteomyelitis, cervical lymph nodes, diffusion-weighted magnetic resonance imaging, magnetic resonance imaging,

2. Introduction

MRI has excellent contrast resolution and its frequently used to diagnose in the head and neck region. The efficacy of MRI in the evaluation of nerve tissues, osteomyelitis of the jaw and cervical lymph nodes has been reported in previous studies.[1-3] Diffusion-weighted imaging (DWI) enables tissue quantification by providing information with respect to the Brownian motion of water, which can facilitate the diagnosis of various lesions, such as benign and malignant tumors, stroke, osteoporosis, and osteomyelitis.[3-12] DWI provides signal contrast utilizing differences in diffusion and movement of water molecules within various tissues, making it possible to detect subtle anomalies. This means changes in tissue structure can be detected at the molecular level. Quantitative evaluation is possible by acquiring the apparent diffusion coefficient (ADC) calculated from diffusion-weighted images with multiple b values. Several studies have evaluated the ADC values calculated from DWI (e.g., osteomyelitis, osteoporosis, and tumors).[5,6,7]

Suppurative osteomyelitis of the jaw is a common maxillofacial disease, defined as a progressive inflammation of the bone and bone marrow. A prominent sign of suppurative osteomyelitis in the lower jaw is mental nerve palsy, also known as Vincent's syndrome.[13,14] During the first stages of infection, bacteria multiply by

inducing inflammatory reaction, resulting in bone edema. The increased intramedullary pressure caused by edema directly compresses the inferior alveolar neurovascular bundle, causing ischemia, promoting thrombosis, and leading to dysfunction or disability of the inferior alveolar nerve (IAN), resulting in Vincent's syndrome.[13,14] Thus, thorough assessment of the IAN affected by osteomyelitis.

The mandibular canal (MC) is a prominent canal within the mandible that envelops the IAN, arteries, and veins. The MC is a prominent canal within the mandible encasing the IAN, artery, and vein. The mandibular foramen is the opening of the MC entering into the mandible.[15,16] The MC is an important landmark to be considered while planning procedures, such as impacted tooth extraction, dental implant placement, bilateral sagittal split osteotomy, apical surgeries, and anesthetic procedures.

About three hundred lymph nodes are situated in the head and neck, and many facilities use the Imaging-based nodal classification[17]. In this classification system, level I corresponds to the submental nodes and submandibular nodes. Levels II correspond to the internal jugular nodes (superior to inferior). Level I and Level II nodes are known to have an increased risk of metastasis to malignant tumors of the oral cavity, nasal passages, and oropharynx. Generally, the 5-year survival rate is extremely low if metastases are found in the cervical lymph nodes, independent of the site of the primary.

In addition, it has been reported that the presence of metastatic lymph nodes on both sides of the neck reduces survival to 25% compared to patients without metastases.[18-21] Since the presence or absence of lymph node metastasis has a great influence on the prognosis, the role of imaging examination such as computed tomography (CT) and magnetic resonance imaging (MRI) in the evaluation of lymph node metastasis is significantly importance. MRI with excellent concentration resolutions the basis for preoperative and postoperative evaluation of patients with lymph node metastasis in the neck region.

However, there are few studies that to assess the MC affected by osteomyelitis and the age-related changes in cervical lymph nodes using ADC values.

The purposes of this study were 1) to evaluate of the MC affected by osteomyelitis using DWI and, 2) to quantitatively assess the age-related changes in ADC values of the normal cervical lymph nodes using DWI.

3. Materials and Methods

3-1. Evaluation of the mandibular canal on inflammatory condition by magnetic resonance imaging.

Subjects

This retrospective study was approved by the institutional review board (EC21-003). This study population consisted of 130 osteomyelitis patients (50 men, 80 women; mean age, 55.7 years; age range, 20–89 years) who visited hospital between April 2013 and March 2020. Osteomyelitis was diagnosed based on the clinical symptoms (fever, malaise, swelling, local redness, pain around soft tissue, and Yumikura and Vincent's symptoms) and typical clinical imaging findings.[13,14] Of the 155 patients initially examined, 10 were excluded because of severe susceptibility artifacts, one owing to a history of radiotherapy, 10 owing to medication history (bisphosphonates and angiogenesis inhibitors), two with a history of cysts in the mandible, and two because of sequestration in the mandible.

Methods

MRI was performed using a 1.5-T superconductive MR unit (Intera Achieva® 1.5 T Nova; Philips Medical Systems, Best, Netherlands) and a 5-channel phased array coil. DWI conditions were as follows: TR/TE = 5100/70, slice thickness, 6 mm; matrix,

256×256 mm; field of view, 250×250 mm; acquisition, 3; and imaging time, 3. An ADC map was created on the MRI console.

The region of interest was set on the slice where the mandibular foramen was observed, and the ADC value of the mandibular foramen was measured on the affected and non-affected sides. The cortical bone, adipose tissue, and muscles were excluded (Fig. 1). The ADC value of the MC was separately recorded and measured by two oral radiology specialists.

Statistical analyses

The intraclass correlation coefficient (ICC) (model 2,1) results were interpreted as follows: values among 0–0.2 indicated slight, 0.21–0.39 minimal, 0.40–0.59 weak, 0.60–0.79 moderate, 0.80–0.90 strong, and > 0.90 perfect agreements.[11]

Non-normality of data was confirmed using the Kolmogorov–Smirnov test. The Wilcoxon signed-rank test was used to compare the ADC values of MC on the affected and non-affected sides. This test was performed using the ADC value of the MC as the criterion variable and disease status as the explanatory variable. The Mann–Whitney U test was used to compare the ADC values of the MC in the male and female groups. This test was performed using the ADC value of the MC as the criterion variable and sex as the explanatory variable. Spearman's correlation coefficients were calculated

using age as the explanatory variable and the ADC value of the MC as the criterion variable. These analyses were performed by SPSS (version 28.0®, IBM Japan Inc., Tokyo, Japan). $P<0.05$ was considered statistically significant.

3-2. Quantitative analysis of age-related changes in the cervical lymph nodes using diffusion-weighted imaging.

Subjects

This retrospective cohort study was approved by the Ethics Committee of university (EC15-12-009-1). The study population consisted of 101 patients (22 men and 79 women, aged 14 to 77 years; mean age, 44.33 years) who had undergone panoramic radiography and MRI scan between April 2018 and November 2020, and those with severe metal artifact, severe periodontitis, apical periodontitis, tumors or cysts of the mandible, hematological disorders, smoking, and osteomyelitis were excluded based on the clinical findings, panoramic radiography, and MRI.

Methods

Panoramic radiography was performed using a panoramic radiography (Veraviewepocs; J. Morita Ltd., Kyoto, Japan) at 1-10 mA and a peak kV of 60-80. MRI was performed using a 1.5-T superconductive MR unit (Intera Achieva® 1.5 T Nova,

Philips Medical Systems, Best, The Netherlands) and a 5-channel phased array coil. EPI-DWI scans were performed using the following parameters: TR/TE = 5100/70; section thickness, 6.0 mm; matrix, 192; FOV, 350 mm; intersection gap, 1.4 mm; imaging time, 3 min 29 s; and b = 0, 1000 s/mm^2. Segmentation and ADC calculation were performed at a dedicated off-line workstation (Philips Medical Systems, Best, The Netherlands). ROIs, with 5 mm diameter, were manually assigned on the ADC map over the mandibular bone marrow on both sides, or just below the first molar to reduce the influence of the anatomical structure. The mandibular tooth germ, canal, root, and cortical bone were excluded (Fig. 9). The ADC values of each participant were independently measured one time and recorded by two oral radiologists on the same slice (K. I., 10 years of experience; H. M., 9 years of experience).

Panotomography was performed using a digital panoramic X-ray system (Veraviewepocs; J. Morita Ltd., Kyoto, Japan) with a setting of 10 mA and a 60-80 kV. MRI was used with a 1.5-T superconductive MR unit (Intera Achieva® 1.5 T Nova; Philips Medical Systems, Best, Netherlands) and a 5-channel phased array coil. Single-shot echo planar-DWI were conducted using the following parameters: TR/TE = 5100/70, 2.0 SENSE factor, 1566 Hz/ pixel bandwidth, 6.0-mm section thickness, 128× 128 acquisition matrix, 256 × 256 reconstruction matrix, 250 × 250-mm FOV,

intersection gap 1.4 mm, 3 number of acquisition, imaging time 3 min 29 s, and b = 0, 1000 s/mm^2. The ADC map was created in the MR console.

The regions of interest (ROIs) were manually assigned on the ADC map over each lymph nodes (Submandibular and superior internal jugular nodes) and (Fig. 8).

1) Submandibular nodes are lying between the hyoid bone and the mylohyoid muscle, and anterior to the back of the submandibular gland.
2) Superior internal jugular nodes are located posterior to the back of the submandibular gland and anterior to the back of the sternocleidomastoid muscle. They lie around the internal jugular vein.

The ADC values of largest bilateral lymph nodes were independently measured one time and recorded by two oral radiologists on the same slice (I. K., 11 years of experience; H. M., 10 years of experience). After the measurement, the ADC values on bilateral sides were averaged.

Statistical analysis

The intraclass correlation coefficient (ICC) (model 2, 1) values were interpreted as follows: <0.5, 0.50–0.75, 0.75–0.90, and >0.90 indicated poor, moderate, good, and excellent reliability, respectively.[11] Spearman's correlation coefficients were calculated using the ADC values of the lymph nodes as the criterion variable and sex and age as

the explanatory variable. These analyses were performed using a statistical package (SPSS version 28.0®, IBM Japan Inc., Tokyo, Japan). Statistical significance was set at $P < .0.05$.

4. Results

4-1. Evaluation of the mandibular canal on inflammatory condition by magnetic resonance imaging.

The ICC for ADC values indicated moderate agreement (ICC=0.69).

In many patients, the ADC values of MC affected by osteomyelitis were higher than those of MC on the non-affected side (Fig. 2). The median ADC value [interquartile range (IQR)] of the MC on the affected side was 1.34 [0.98–1.45] $\times 10^{-3}$ mm^2/s and that of the MC on the non-affected side was 1.12 [0.86–1.22] $\times 10^{-3}$ mm^2/s (Table 1). Box-and-whisker plot shows that the median ADC values of MC on the affected side were higher than those of MC on the non-affected side (Fig. 3).

The median ADC value [IQR] of the MC for affected side groups was 1.35 [1.22–1.45] $\times 10^{-3}$ mm^2/s in men and 1.21 [1.06–1.34] $\times 10^{-3}$ mm^2/s in women. No significant differences in the median ADC values of the MC for affected side groups were observed between the sexes ($P = 0.24$, Fig. 4). The median ADC value [IQR] of the MC for non-affected side groups was 1.29 [1.15–1.45] $\times 10^{-3}$ mm^2/s in men and 1.20 [1.08–1.34] $\times 10^{-3}$ mm^2/s in women. No significant differences in the median ADC values of the MC for non-affected side groups were observed between the sexes ($P = 0.41$, Fig. 5).

The median ADC values of the MC affected by osteomyelitis were as follows: 1.10 (20–29 years; n = 2), 1.27 (30–39 years; n = 5), 1.28 (40–49 years; n = 27), 1.36 (50–59

years; n = 18), 1.33 (60–69 years; n = 28), 1.36 (70–79 years; n = 37), and 1.23 (80–89 years; n = 13), according to age. There was no significant correlation between patient age and the ADC value of the MC affected by osteomyelitis (r=-0.013, *P*=0.88, Fig. 6). Moreover, the median ADC values of the non-affected side were as follows: 1.12 (20–29 years; n = 2), 0.974 (30–39 years; n = 5), 1.23 (40–49 years; n = 27), 1.21 (50–59 years; n = 18), 1.23 (60–69 years; n = 28), 1.20 (70–79 years; n = 37), and 1.18 (80–89 years; n = 13), according to age. There was no significant correlation between patient age and the ADC value of MC on the non-affected side (r=-0.01, *P*=0.906, Fig. 7).

4-2. Quantitative analysis of age-related changes in the cervical lymph nodes using diffusion-weighted imaging

Good agreement in the ADC values ($\times 10^{-3}$ mm^2/s) of the bone marrow (ICC = 0.791) was found. The mean ADC value of submandibular nodes for all the age groups was 0.88±0.15 $\times 10^{-3}$ mm^2/s in men and 0.83 ± 0.12 $\times 10^{-3}$ mm^2/s in women (*P* = 0.211) (Table 1). Moreover, the mean ADC value of superior internal jugular nodes for all the age groups was 0.90±0.14 $\times 10^{-3}$ mm^2/s in men and 0.91 ± 0.16 $\times 10^{-3}$ mm^2/s in women (*P* = 0.857) (Table 2). Significant difference was not observed in the mean ADC value of each node between men and women group.

The mean ADC values of the submandibular nodes were as follows: 0.97± 0.12 (14–19 years; n = 10), 0.91± 0.11 (20–29 years; n = 17), 0.9± 0.13 (30–39 years; n = 13), 0.81± 0.11 (40–49 years; n = 21), 0.79± 0.09 (50–59 years; n = 14), 0.79± 0.13 (60–69 years; n = 18), and 0.75± 0.11 (70–77 years; n = 8), according to age ($r = -0.564$, $P < 0.01$) (Table 2). The mean ADC values of the superior internal jugular nodes were as follows: 1.02± 0.16 (15–19 years; n = 10), 0.99± 0.17 (20–29 years; n = 17), 0.94± 0.12 (30–39 years; n = 13), 0.86 ± 0.13 (40–49 years; n = 21), 0.88 ± 0.13 (50–59 years; n = 14), 0.86 ± 0.12 (60–69 years; n = 18), and 0.76 ± 0.08 (70–79 years; n = 8), according to age ($r = -0.518$, $P< 0.01$) (Table 3). Thus, the ADC values showed a significant negative correlation with age (Fig. 9 and 10). Furthermore, depending on the group, ADC values tended to be higher in the superior internal jugular nodes than in the submandibular nodes (Fig. 11).

5. Discussion

5-1. Evaluation of the mandibular canal on inflammatory condition by magnetic resonance imaging.

This study demonstrated that the median ADC value of the MC on the affected side was higher than that of the MC on the non-affected side. Furthermore, ADC values were significantly higher in men than in women and did not correlate with age.

In the MC, the IAN runs anteriorly along the inferior alveolar artery, vein, and lymphatic vessels, collectively known as the inferior alveolar neurovascular bundle. IAN injuries can occur because of surgical errors by clinicians, dental infections, inflammatory diseases, and malignancies.[12,22,23] Damage to the MC can result in various complications including altered or loss of sensation, numbness, and pain.

DWI of the nervous system has been shown to be useful for determining diagnosis and clinical status. In the brain, DWI is used to assess gray and white matter as well as to diagnose hyperacute stroke and tumors.[5-7] Studies have evaluated the inferior alveolar neurovascular bundle in the maxillofacial area using diffusion-weighted or tensor imaging.[24-27]

In this study, the median ADC values of MC on the affected and non-affected sides were 1.34×10^{-3} mm^2/s and 1.12×10^{-3} mm^2/s, respectively. Thus, the median ADC value of the affected side was higher than that of the non-affected side. Kotaki *et al.* reported

that the mean ADC value of the MC in normal cases was $1.02\pm0.24\times10^{-3}$ mm^2/s.[24] Moreover, Ozgen et al. reported that inflammation causes an increase in extracellular fluid levels, resulting in an increase in the ADC value.[28] Thus, a possible explanation for this result is that denaturation of the nerve fibers and arteriovenous tissue causes a change in the interstitial space, and the diffusivity of water molecules increases. This study, however, has some limitations. The study was of a retrospective nature. Moreover, it was not possible to measure ADC values in patients with severe image distortions caused by susceptibility artifacts. Currently, only preliminary results are available, and further studies are required to elucidate the role of DWI.

5-2. Quantitative analysis of age-related changes in the cervical lymph nodes using diffusion-weighted imaging

Lymph nodes shows that generally tend to decrease in number and size with age.[29] And, changes in lymphatic flow due to age-related fat degeneration of lymph nodes and decreased lymphatic function have been reported.[29-32] This change in lymphatic flow is thought to be due to decreased tissue turgor pressure, which is associated with the destruction of elastic tissue, decreased blood flow, and changes in fat composition.[32] These changes are no exception to the cervical lymph nodes such as the submandibular

nodes and superior internal jugular nodes. The submandibular lymph nodes and the superior internal jugular nodes are the lymphatic drainage pathways for lymph from the oral region. In particular, the submandibular lymph nodes are recognized as a nodes where squamous cell carcinoma often metastasizes. Correct assessment of these cervical lymph nodes is especially important for patients with malignant tumor in maxillofacial area because it is useful for treatment planning and prognosis prediction.[33,34] Its correct assessment also prevents patients with reactive lymphadenopathy from unnecessary treatment.[35] Evaluation of cervical lymph nodes such as size, shape, and necrosis has been made possible by the latest imaging techniques, but there are few reports of evaluation of internal properties of lymph nodes by aging using DWI.

DWI can be used to visualize the random movement of water protons inside and outside cells in the body wile by reflecting the microstructure and physiological state of the tissue independent of T1 and T2. Several studies have reported on the role of DWI in characterization of cervical lymph nodes.[9,34,35] However, to the best of knowledge, there are no reports of quantitative assessment of age-related changes in the cervical lymph nodes using DWI. This study was considered important for accurate Differential diagnosis of lymph nodes, as age-related changes in ADC values can affect the quantitative assessment of cervical lymph nodes using DWI.

Razek et al reported that the mean ADC value of metastatic lymph nodes was lower than that of benign ones, with a cutoff value of 1.38×10^{-3} mm^2/ s, and higher sensitivity and specificity were obtained.[35] This metastatic lymph node has a decrease in ADC, which may be due to cell hyperplasia, increased nuclear-to-cytoplasmic ratio, and the effects of perfusion.[36] Conversely, Sumi et al reported that metastatic lymph nodes have significantly higher mean ADC values than benign lymph node tumors.[21] This different result may be due to such as choice of the b values, ROI selection, age, and sex. This study revealed a statistically significant negative correlation between the mean ADC values of each lymph nodes and age. It is possible that age-related decreased lymphatic flow and fatty degeneration reduced perfusion and diffusion resulting affected ADC values. In addition, this study found that ADC values tend to be higher in the superior internal jugular lymph nodes than that of submandibular nodes in each age group. It may be due to more lymphatic drainage from the maxillofacial area.

6. Conclusion

The present study found that 1) the ADC value of MC affected by osteomyelitis was significantly higher than those of the MC non-affected side, 2) the normal ADC values of cervical lymph nodes exhibited significant negative correlation with increasing age. These results suggested that the efficacy of DWI in the head and neck region.

6. References

1. Kaneda T, Minami M, Ozawa K, Akimoto Y, Okada H, Yamamoto H, Suzuki H, Sasaki Y. Magnetic resonance appearance of bone marrow in the mandible at different ages. Oral Surg Oral Med Oral Pathol Oral Radiol and Endod. 1996;82: 229–233.
2. Martín Noguerol T, Barousse R, Socolovsky M, Luna A. Quantitative magnetic resonance (MR) neurography for evaluation of peripheral nerves and plexus injuries. Quant Imaging Med Surg. 2017;7:398–421.
3. Lee K, Kaneda T, Mori S, Minami M, Motohashi J, Yamashiro M. Magnetic resonance imaging of normal and osteomyelitis in the mandible: assessment of short inversion time inversion recovery sequence. Oral Surg Oral Med Oral Pathol Oral Radiol Endod. 2003;96:499–507.
4. Muraoka H, Hirahara N, Ito K, Okada S, Kondo T, Kaneda T. Efficacy of diffusion-weighted magnetic resonance imaging in the diagnosis of osteomyelitis of the mandible. Oral Surg Oral Med Oral Pathol Oral Radiol. 2022;133:80–87.
5. Tien R, Felseberg G, Friedman H, Brown M, MacFall J. MR imaging of high-grade cerebral gliomas: value of diffusion-weighted echoplanar pulse sequences. AJR Am J Roentgenol. 1994;162:671–677.

6. Kimura K, Minematsu K, Koga M, Arakawa R, Yasaka M, Yamagami H, Nagatsuka K, Naritomi H, Yamaguchi T. Microembolic signals and diffusion-weighted MR imaging abnormalities in acute ischemic stroke. AJNR Am J Neuroradiol. 2011;22: 1037–1042.

7. Kim YJ, Chang KH, Song IC, Kim HD, Seong SO, Kim YH, Han MH. Brain abscess and necrotic or cystic brain tumor: discrimination with signal intensity on diffusion-weighted MR imaging. AJR Am J Roentgenol.1998;171:1487–1490.

8. Vanagundi R, Kumar J, Manchanda A, Mohanty S, Meher R. Diffusion-weighted magnetic resonance imaging in the characterization of odontogenic cysts and tumors. Oral Surg Oral Med Oral Pathol Oral Radiol. 2022;130: 447–454.

9. Koyama H, Yoshihara H, Kotera M, Tamura T, Sugimura K. The quantitative diagnostic capability of routine MR imaging and diffusion-weighted imaging in osteoporosis patients. Clin Imaging. 2013;37:925–929.

10. Wang P, Yang JY, Yu O, Ai S, Zhu W. Evaluation of solid lesions affecting masticator space with diffusion-weighted MR imaging. Oral Surg Oral Med Oral Pathol Oral Radiol Endod. 2010;109:900–907.

11. Koo TK, Li MY. A guideline of selecting and reporting intraclass correlation coefficients for reliability research. J Chiropr Med. 2016;15(2):155–163.

12. Yamamoto R, Nakamura A, Ohno K, Michi K. Relationship of the mandibular canal to the lateral cortex of the mandibular ramus as a factor in the development of neurosensory disturbance after bilateral sagittal split osteotomy. J Oral Maxillofac Surg. 2022;60:490–495.

13. Baltensperger M, Eyrich G. Osteomyelitis of the Jaws. Definition and classification. Osteomyelitis of the jaws. Springer.Berlin Heidelberg. 2009;5–56.

14. Kremers H, Nwojo M, Ransom J, Wood-Wentz C, Melton LJ 3rd. Huddleston PM 3rd. Wood-Wentz C, Melton LJ 3rd, Huddleston PM 3rd: Trends in the epidemiology of osteomyelitis: a population-based study,1969 to 2009. J Bone Joint Surg Am. 2015;97:837–845.

15. Movahhedian N, Sardarian A, Hosseini A, Momeni Danaei S, Hamedani S. Skeletal maturation, and the location of the mandibular foramen within the ramus mandibulae. J Orofac Orthop. 2022;83:56–64.

16. Haas LF, Dutra K, Porporatti AL, Mezzomo LA, De Luca Canto G, Flores-Mir C, Corrêa M. Anatomical variations of mandibular canal detected by panoramic radiography and CT: a systematic review and meta-analysis. Dentomaxillofac Radiol. 2016;45:20150310.

17. Som PM, Curtin HD, Mancuso AA. Imaging-based nodal classification for evaluation of neck metastatic adenopathy. AJR Am J Roentgenol. 2000;174(3):837–844.

18. Farr HW, Goldfarb PM, Farr CM. Epidem,oid carcinoma of the mouth and pharynx at Memorial Sloan Kettering Cancer Center 1965 to 1969. Am J Surg. 1980;140: 563–567.

19. Spiro RH. The management of neck nodes in head and neck cancer: a surgeon's view. Bull N V Acad Med. 1985;61:629–637.

20. Som PM. Detection of metastasis in cervical lymph nodes: CT and MR criteria and differential diagnosis. AJR. 1992;158:961–969.

21. Sumi M, Sakihama N, Sumi T, Morikawa M, Uetani M, Kabasawa H, Shigeno K, Hayashi K, Takahashi H, Nakamura T. Discrimination of metastatic cervical lymph nodes with diffusion-weighted MR imaging in patients with head and neck cancer. AJNR Am J Neuroradiol. 2003;24(8):1627–1634.

22. Hiraoka Y, Akashi M, Wanifuchi S, Kusumoto J, Shigeoka M, Hasegawa T, Terashi H, Komori T. Association between pain severity and clinicohistopathologic findings in the mandibular canal and inferior alveolar nerve of patients with advanced

mandibular osteoradionecrosis. Oral Surg Oral Med Oral Pathol Oral Radiol. 2018;126:264–271.

23. Suzuki N, Kuribayashi A, Sakamoto K, Sakamoto J, Nakamura S, Watanabe H, Harada H, Kurabayashi T. Diagnostic abilities of 3T MRI for assessing mandibular invasion of squamous cell carcinoma in the oral cavity: comparison with 64-row multidetector CT. Dentomaxillofac Radiol. 2019;48:20180311.
24. Kotaki S, Sakamoto J, Kretapirom K, Supak N, Sumi Y, Kurabayashi T. Diffusion tensor imaging of the inferior alveolar nerve using 3T MRI: a study for quantitative evaluation and fibre tracking. Dentomaxillofac Radiol. 2016;45:1–7.
25. Muraoka H, Hirahara N, Ito K, Tokunaga S, Okada S, Otsuka K, Komatsu T, Kondo T, Kaneda T. Quantitative assessment of the age-related change of inferior alveolar neurovascular bundle using diffusion weighted magnetic resonance imaging.Int J Oral-Med Sci. 2021;20:31–36.
26. Gauvain KM, McKinstry RC, Mukherjee P, Perry A, Neil JJ, Kaufman BA. Evaluating pediatric braintumor cellularity with diffusion-tensor imaging. AJR Am J Roentgenol. 2001;177:449–454.
27. Manoliu A, Ho M, Piccirelli M, Nanz D, Filli L, Dappa E, Liu W, Ettlin DA, Bpss A, Andreisek G, Kuhn FP. Simultaneous multislice readout-segmented echo planar

imaging for accelerated diffusion tensor imaging of the mandibular nerve: A feasibility study. J Magn Reson Imaging. 2017;46:663–677.

28. Ozgen B, Oguz KK, Cila A. Diffusion MR imaging features of skull base osteomyelitis compared with skull base malignancy. AJNR Am J Neuroradiol. 2011;32:179–184.

29. Robbins KT, Clayman G, Levine PA, Medina J, Sessions R, Shaha A, Som P, Wolf GT. American Head and Neck Society; American Academy of Otolaryngology--Head and Neck Surgery. Neck dissection classification update: revisions proposed by the American Head and Neck Society and the American Academy of Otolaryngology-Head and Neck Surgery. Arch Otolaryngol Head Neck Surg. 2002; 128(7):751–758.

30. Luscieti P, Hubschmid T, Cottier H, Hess MW, Sobin LH. Human lymph node morphology as a function of age and site. J Clin Pathol. 1980;33:454–461.

31. Moon HJ, Suh JS, Lee SH. Magnetic Resonance appearance of normal popliteal lymph nodes: location and relationship of number, fatty changes, and size of the lymph nodes with aging. J Korean Radiol Soc. 2002;47:665–671.

32. Conway WC, Faries MB, Nicholl MB, Terando AM, Glass EC, Sim M, Morton DL. Age-related lymphatic dysfunction in melanoma patients. Ann Surg Oncol. 2009 Jun;16(6):1548–1552.

33. Ying M, Ahuja A, Brook F. Sonographic appearances of cervical lymph nodes: variations by age and sex. J Clin Ultrasound. 2002;30(1):1–11.

34. Kennedy C, Bastiaens MT, Bajdik CD, Willemze R, Westendorp RG, Bouwes Bavinck JN. Effect of smoking and sun on the aging skin. J Invest Dermatol. 2003; 120(4):548–554.

35. Abdel-Razek AA, Soliman NY, Elkhamary S, Alsharaway MK, Tawfik A. Role of diffusion-weighted MR imaging in cervical lymphadenopathy. Eur Radiol. 2006; 16:1468–1477.

36. Wang J, Takashima S, Takayama F, Kawakami S, Saito A, Matsushita T, Momose M, Ishiyama T. Head and neck lesions: characterization with diffusion-weighted echo-planar MR imaging. Radiology. 2001;220(3):621–630.

8. Figures and legends

Fig. 1 Apparent diffusion coefficient (ADC) map of the mandibular foramen

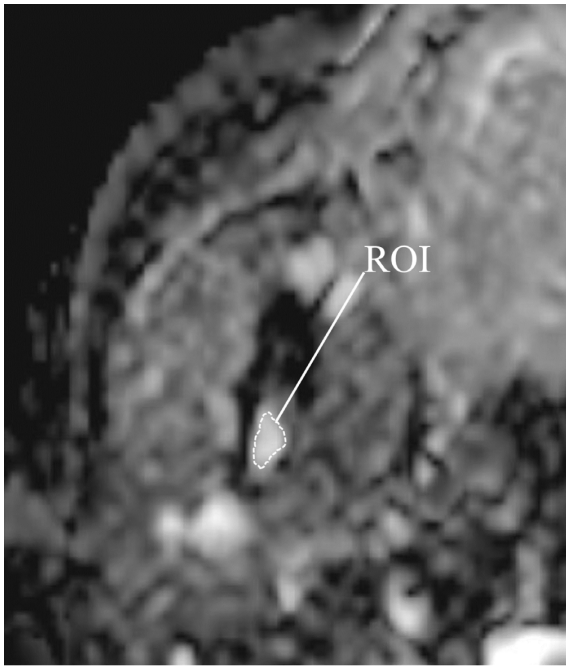

The regions of interest manually drawn on the apparent diffusion coefficient map at the mandibular foramen site. The cortical bone and surrounding tissues were excluded.

Fig. 2 The apparent diffusion coefficient (ADC) values of the mandibular canal (MC) on the affected and non-affected sides in a 60-year-old man

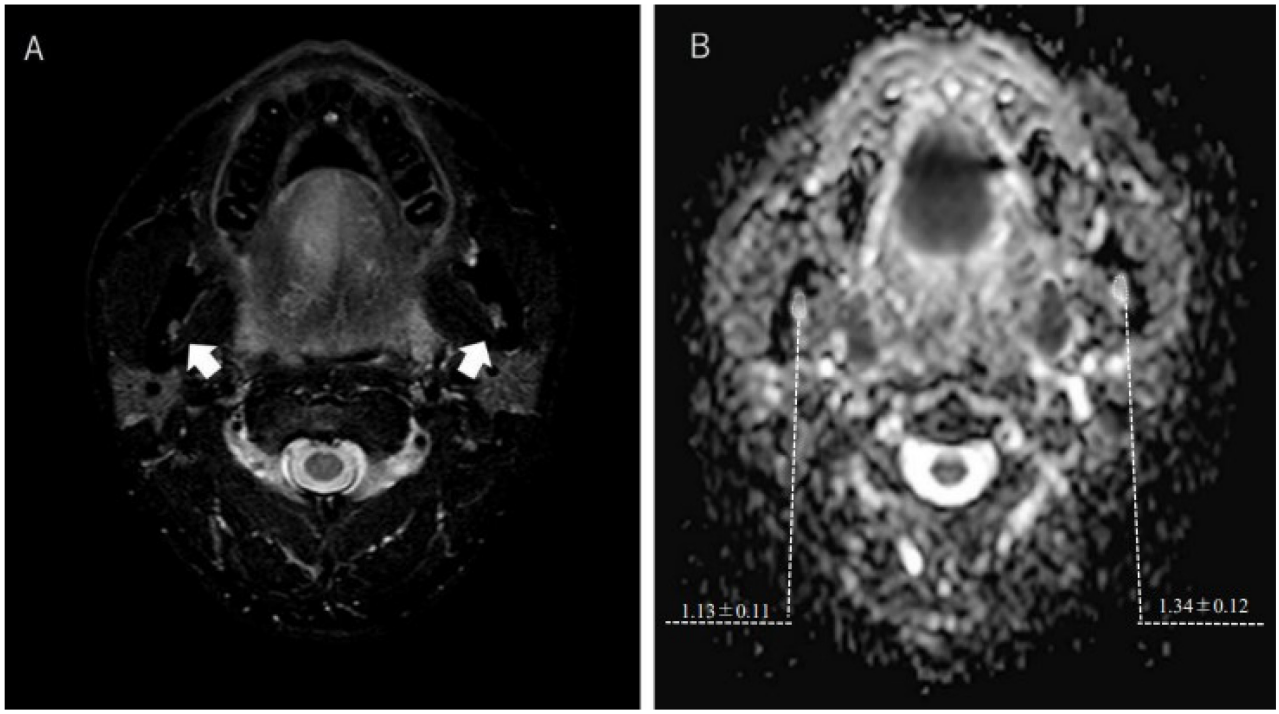

A, B: Axial short tau inversion recovery and diffusion-weighted images of the MC (arrows and regions of interest). The median ADC value of the MC affected by osteomyelitis was 1.34×10^{-3} mm^2/s, whereas that of the MC on the non-affected side was 1.13×10^{-3} mm^2/s.

Fig. 3 Comparative median apparent diffusion coefficient (ADC) values of the mandibular canal regions affected and non-affected by osteomyelitis

The ADC values of MC affected by osteomyelitis were higher than those of MC on the non-affected side. The median ADC value [interquartile range (IQR)] of the MC on the affected side was 1.34 [0.98–1.45] $\times 10^{-3}$ mm^2/s and that of the MC on the non-affected side was 1.12 [0.86–1.22] $\times 10^{-3}$ mm^2/s.

Fig. 4 Box-and-whisker plot indicating the relationship between sex and apparent diffusion coefficient (ADC) value of the mandibular canal affected by osteomyelitis

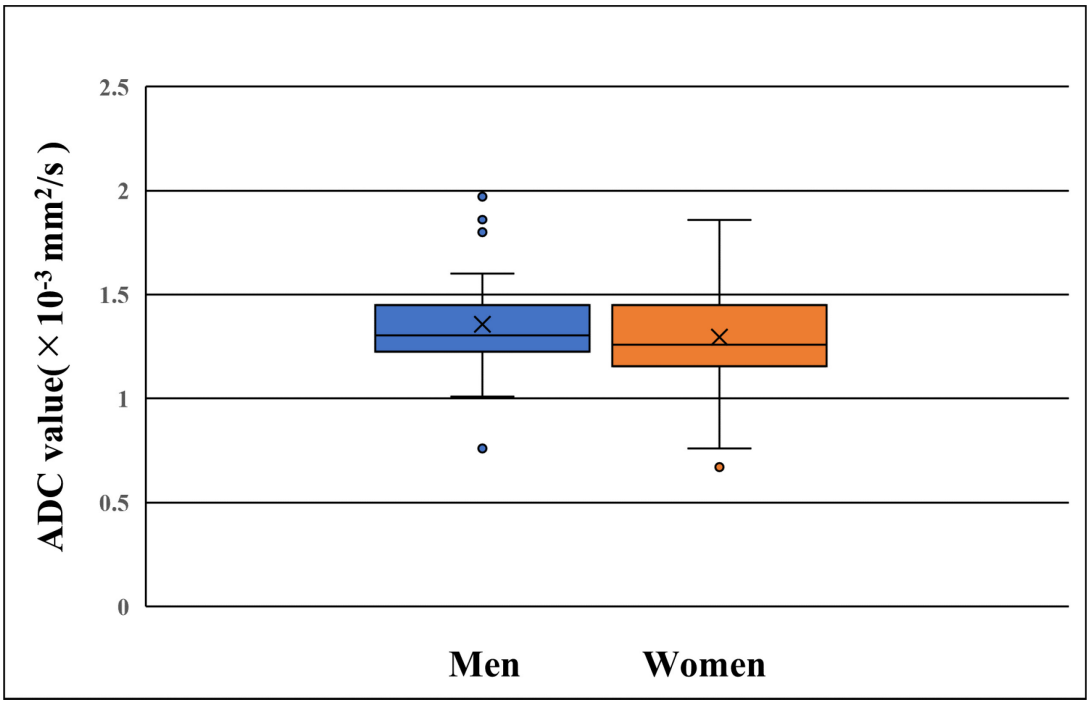

The median ADC value [interquartile range (IQR)] of the MC for affected side groups was 1.35 [1.22–1.45] $\times 10^{-3}$ mm^2/s in men and 1.21 [1.06–1.34] $\times 10^{-3}$ mm^2/s in women. No significant differences in the median ADC values of the MC for affected side groups were observed between men and women group ($P = 0.24$).

Fig. 5 Box-and-whisker plot indicating the relationship between sex and apparent diffusion coefficient (ADC) value of the mandibular canal on non-affected side

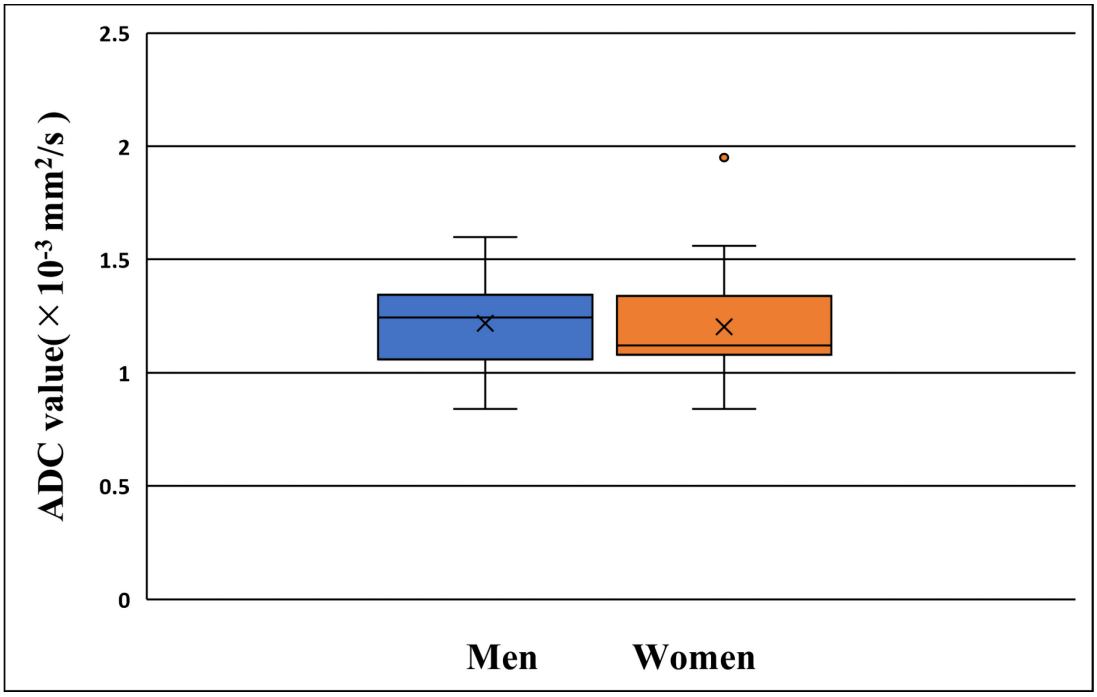

The median ADC value [interquartile range (IQR)] of the MC for non-affected side groups was 1.29 [1.15–1.45] $\times 10^{-3}$ mm^2/s in men and 1.20 [1.08–1.34] $\times 10^{-3}$ mm^2/s in women. No significant differences in the median ADC values of the MC for non-affected side groups were observed between the men and women group ($P = 0.41$).

Fig. 6 Scatter plot showing the relationship between the apparent diffusion coefficient (ADC) of the mandibular canal affected by osteomyelitis and age.

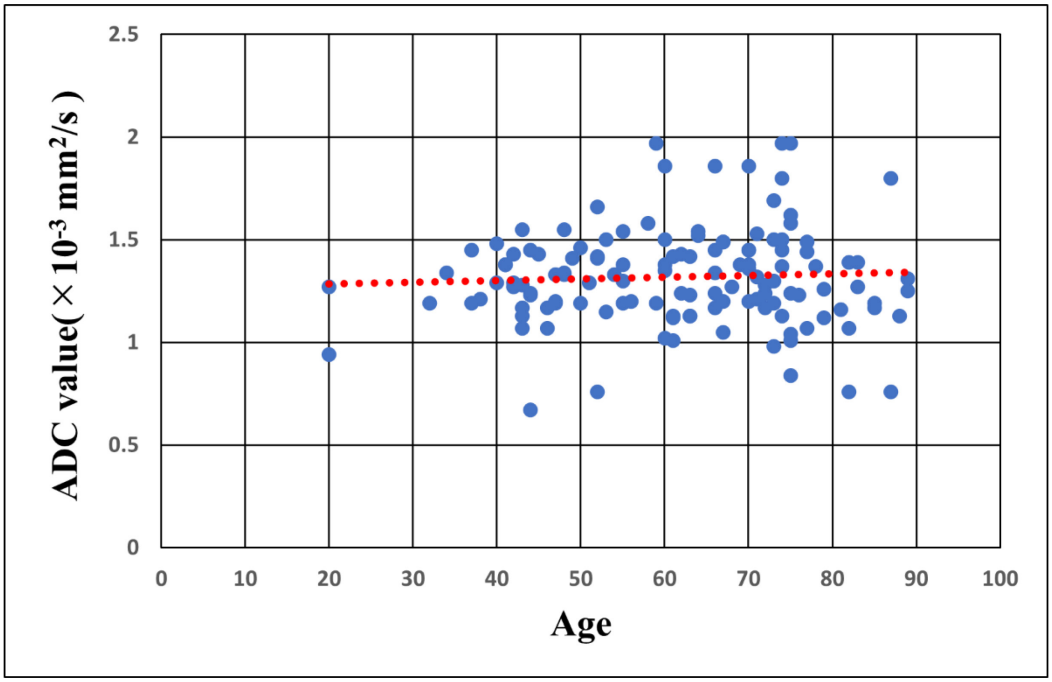

There was no significant correlation between patient age and the ADC value of the MC affected by osteomyelitis (r=-0.013, *P*=0.88).

Fig. 7 Scatter plot showing the relationship between the apparent diffusion coefficient (ADC) of the mandibular canal on non-affected side and age.

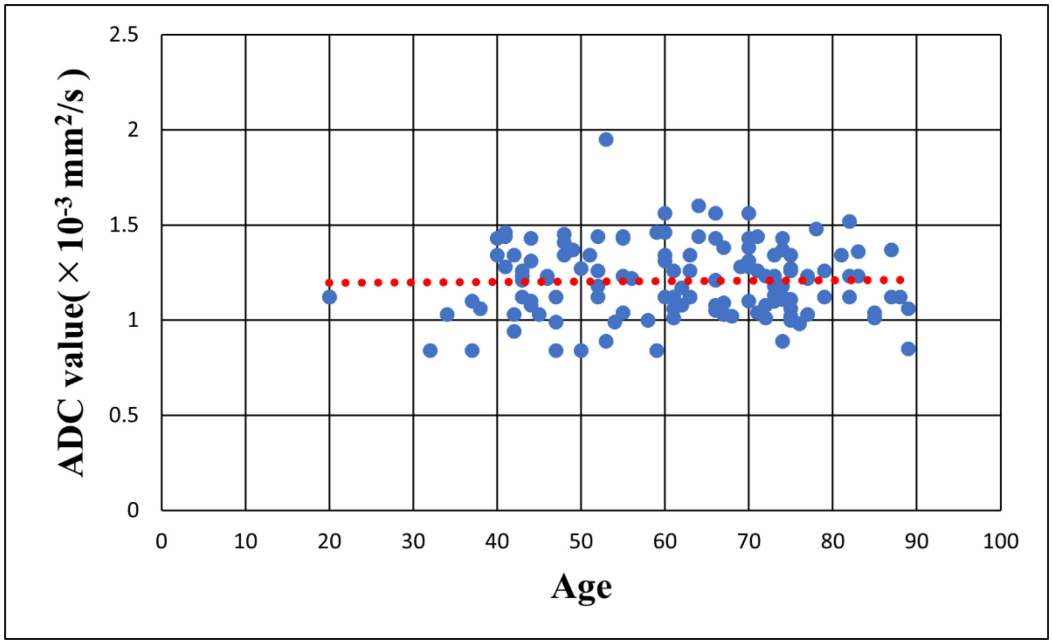

There was no significant correlation between patient age and the ADC value of MC on the non-affected side (r=-0.01, *P*=0.906).

Fig. 8 Apparent diffusion coefficient (ADC) map of submandibular and superior internal jugular nodes

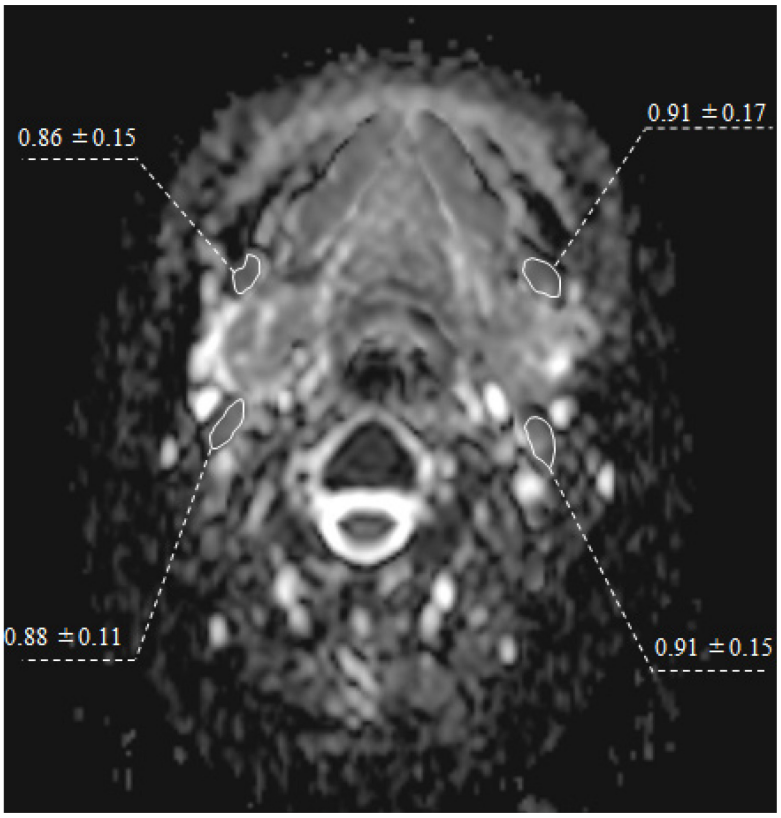

The regions of interest (ROIs) were manually assigned on the apparent diffusion coefficient (ADC) map over each lymph nodes on both sides.

Fig. 9 Relationship between the apparent diffusion coefficient (ADC) of the submandibular nodes and age

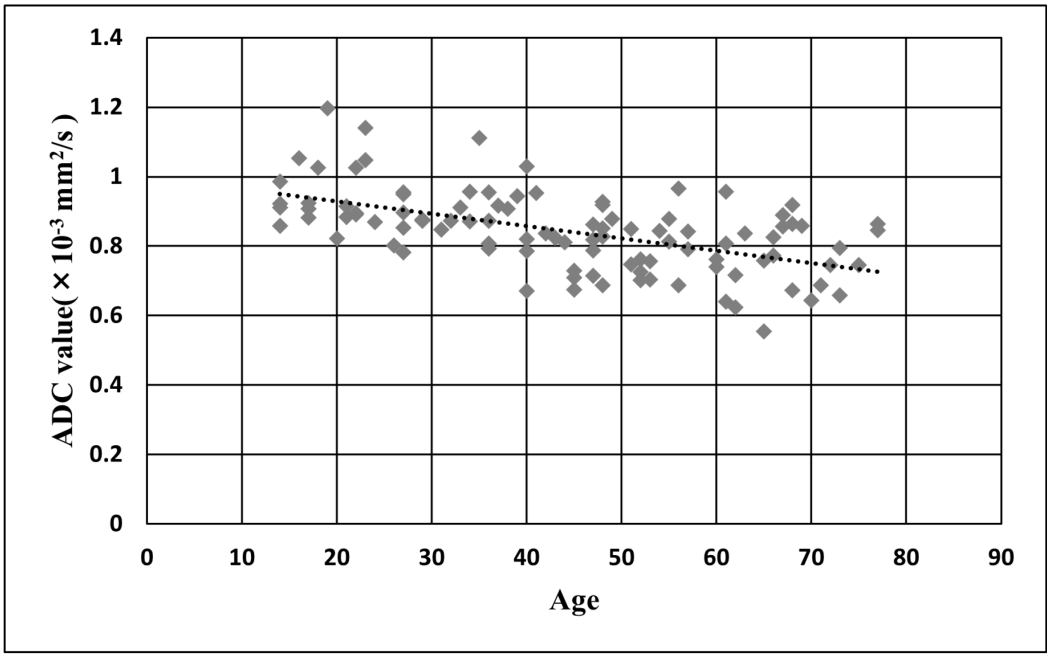

Scatter plot showed a significant negative correlation between the ADC values of submandibular nodes and age.

Fig. 10 Relationship between the apparent diffusion coefficient (ADC) of the submandibular nodes and age

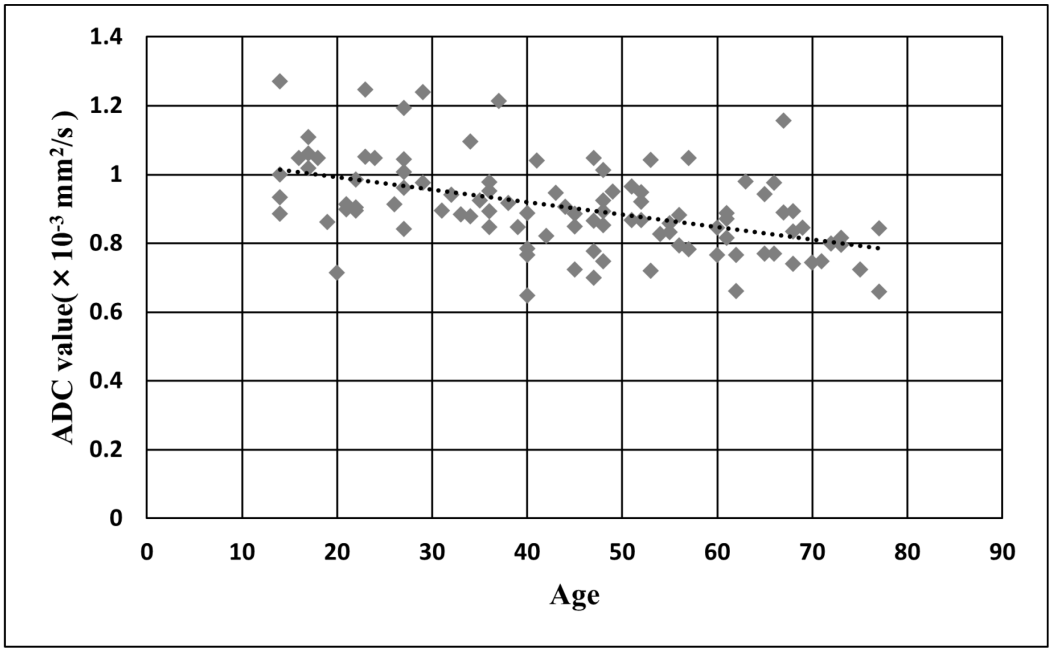

Scatter plot showed a significant negative correlation between the ADC values of superior internal jugular nodes and age.

Fig. 11 Box-and-whisker plot of the ADC values of lymph nodes in each age group

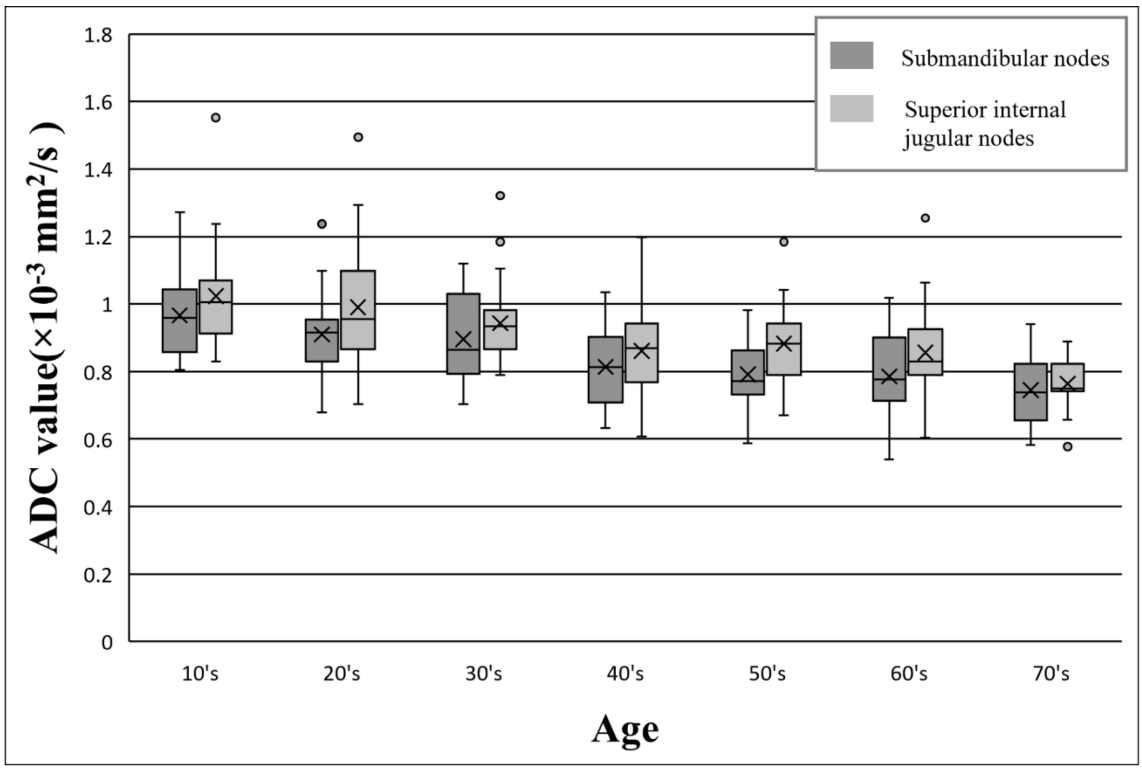

The ADC values tended to be higher in the superior internal jugular nodes than in the submandibular nodes.

9. Table

Table 1 Median apparent diffusion coefficient (ADC) values of the mandibular canal (MC) in each state

	Affected side (n=130)	Non-affected side (n=130)
Median ADC value of the mandibular canal [IQR] ($\times 10^{-3}$ mm^2/s)	1.34 [0.98–1.45]	1.12 [0.86–1.22]

NOTE: ADC= Apparent diffusion coefficient, IQR = Interquartile range

The ADC values of MC affected by osteomyelitis were higher than those of MC on the non-affected side.

Table 2 Mean ADC values of each lymph nodes

	Number of patients (n)		
	Men (n=22)	Women (n=79)	***P*-value**
Mean ADC value of the submandibular nodes ($\times 10^{-3}$ mm^2/s ±SD)	0.88±0.15	0.83±0.12	*P*=.0211
Mean ADC value of the superior internal jugular nodes ($\times 10^{-3}$ mm^2/s ±SD)	0.90±0.14	0.91±0.16	*P*=.0857

NOTE: ADC= Apparent diffusion coefficient, SD= Standard deviation

No significant differences in the mean ADC values of the submandibular nodes were observed between the men and women group. No significant differences in the mean ADC values of the superior internal jugular nodes were observed between the men and women group.

Table 3 ADC values of each lymph nodes in different age

Age groups (n= Number of patients)	ADC value of submandibular nodes (± SD×10^{-3} mm^2/s)	ADC value of superior internal jugular nodes (± SD×10^{-3} mm^2/s)
14～19 (n=10)	0.97± 0.12	1.02± 0.16
20～29 (n=17)	0.91± 0.11	0.99± 0.17
30～39(n=13)	0.9± 0.13	0.94± 0.12
40～49(n=21)	0.81± 0.11	0.86 ± 0.13
50～59(n=14)	0.79± 0.09	0.88 ± 0.13
60～69(n=18)	0.79± 0.13	0.86 ± 0.12
70～77(n=8)	0.75± 0.11	0.76 ± 0.08
r	-0.564**	-0.518**

NOTE: ADC= Apparent diffusion coefficient, SD= Standard deviation

The ADC values showed a significant negative correlation with age, in each lymph nodes.